CONTROLS ON RESERVOIR QUALITY OF THE NANUSHUK FORMATION (ALBIAN–CENOMANIAN), NORTH SLOPE, ALASKA

Kenneth P. Helmold[1] and David L. LePain[2]

[1]Alaska Division of Oil & Gas, 550 W. 7th Ave., Anchorage, AK; current contact: helmold@alaskan.com [2]Alaska Division of Geological & Geophysical Surveys, 3354 College Rd., Fairbanks, AK

ABSTRACT

Recent hydrocarbon discoveries in the Albian–Cenomanian Nanushuk Formation on the North Slope of Alaska have revived interest in exploration of the Colville basin. The Nanushuk forms a segment of the Brookian sequence and together with the genetically related Torok Formation comprises part of a giant clinothem filling the western two-thirds of the basin. It consists of a succession of intertonguing marine and nonmarine strata interpreted as marine shelf, deltaic, strandplain, and fluvial deposits. Deposition occurred in two deltaic complexes, one sourced from large drainage basins extending west of present-day Arctic Alaska, the other from smaller catchment areas with headwaters in the ancestral Brooks Range to the south.

The Nanushuk Formation consists of medium- to very fine-grained lithic sandstone and siltstone comprised largely of monocrystalline and polycrystalline quartz, chert, and argillaceous sedimentary and metasedimentary rock fragments. With progressive burial and compaction, ductile deformation of the argillaceous detritus is the principal mechanism of porosity and permeability loss in the sandstone. Cements are a minor component and have minimal effect on diagenesis of the strata. Reservoir quality varies extensively across the North Slope and understanding the factors controlling reservoir potential is a critical aspect of recent exploration programs.

Two groups of sandstone and siltstone are recognized based on differences in reservoir quality: a low-porosity group with maximum porosity less than 20 percent, and a high-porosity group with higher porosity values for a given permeability and maximum porosity exceeding 30 percent. Variation in reservoir quality within each group is delimited by depositional texture which is a primary, local control. The disparity between the groups results from differences in the maximum burial depth (Dmax) the rocks experienced which is a secondary, regional control. Linear regression models for porosity–Dmax and permeability–Dmax relations enable forecasting the reservoir potential of Nanushuk sandstone and siltstone containing only minor cement.

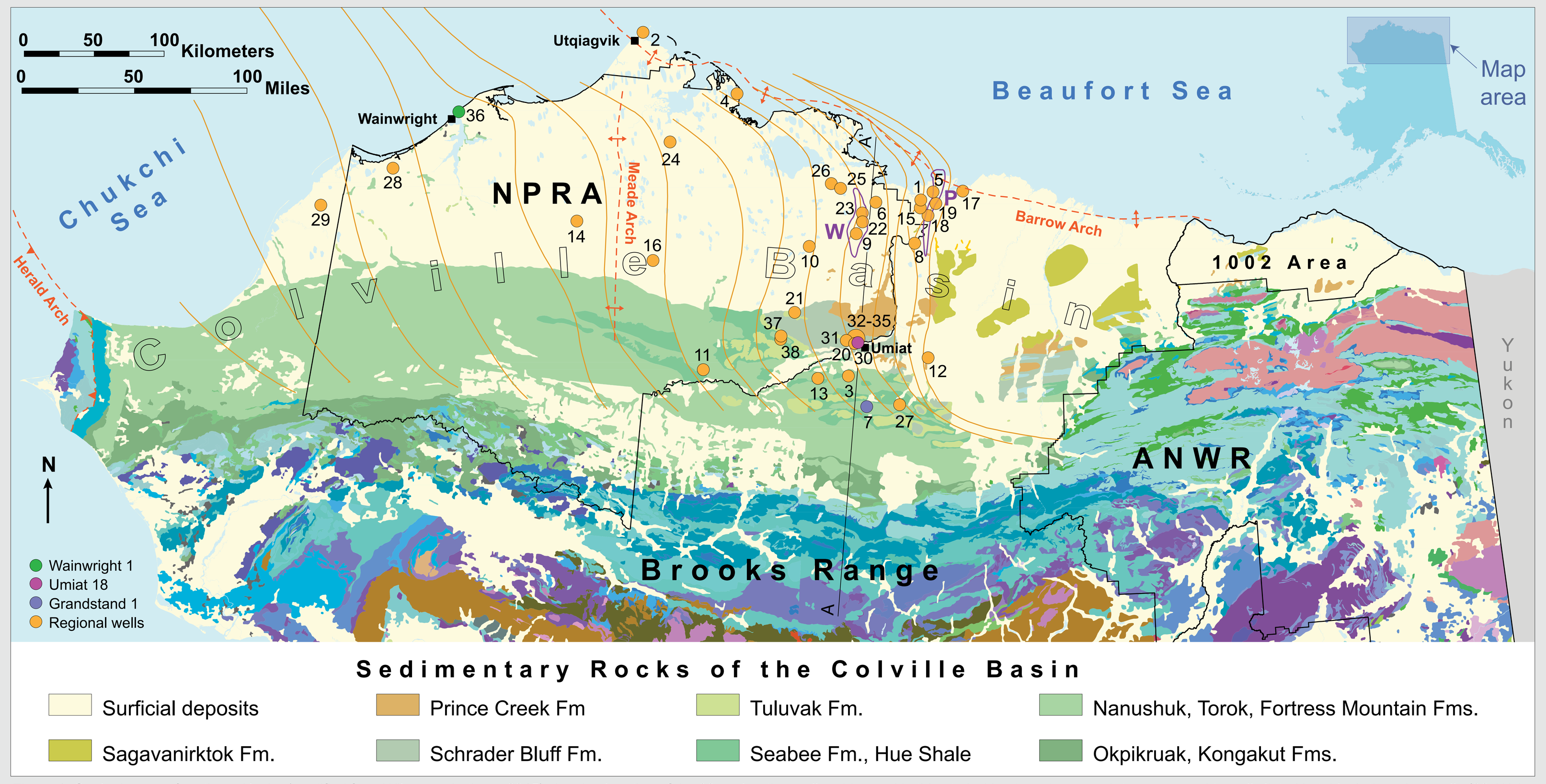

Figure 1. Geologic map of northern Alaska (modified from Wilson and others, 2015) showing location of the 38 exploration wells addressed in this study. Numbered orange dots correspond to wells listed in table 1; three key wells (36–Wainwright 1, 30–Umiat 18, and 7–Grandstand 1) are highlighted. Purple polygons show the locations of the Willow–West Willow (W) and Pikka–Horseshoe–Narwhal (P) accumulations. Orange lines delineate the approximate locations of Nanushuk lowstand shelf margins (Houseknecht, 2019). AA' line depicts location of cross section in fig. 4. For descriptions of geologic units in the Brooks Range see Wilson and others, 2015.

Table 1. Exploration and test wells for which modal data, routine core analyses, and estimates of removed Tertiary overburden are available for Nanushuk Formation. Abbreviation: MD = measured depth.

No.	Operator	Well	API	Top Zone (MD, ft)	Base Zone (MD, ft)	N	Erosion (ft)
1	Arco	Alpine 1	50103202110000	4046.00	4535.00	4	1176
2	US Navy	Barrow Core Test 1	50023100050000	169.00	194.00	6	2725
3	Arco	Big Bend 1	50287200110000	1100.00	2840.00	9	8002
4	Husky	E Simpson 2	50279200070000	2387.00	2398.00	9	1785
5	Arco	Fiord 2	50103202010000	4828.00	6650.00	2	844
6	US Navy	Fish Creek 1	50103100010000	2923.00	3032.90	7	1103
7	US Navy	Grandstand 1	50057100010000	227.50	2512.00	145	8084
8	Armstrong	Horseshoe 1	50103207510000	4332.50	4873.97	149	1728
9	Phillips	Hunter A	50103204050000	3625.00	3652.00	7	2068
10	Husky	Inigok 1	50279200030000	2632.00	3081.90	7	3223
11	US Navy	Knifeblade 1	50119100120000	312.00	1490.00	6	6777
12	BP	Kuparuk Unit 1	50287100180000	5529.00	5930.00	9	7090
13	Sinclair	Little Twist Unit 1	50287100220000	942.00	3611.00	4	8895
14	US Navy	Meade 1	50163100020000	1795.00	2950.00	2	4560
15	Arco	Nanuk 2	50103203320000	4796.00	4828.00	3	1381
16	US Navy	Oumalik Test 1	50119100050000	916.00	2758.30	17	4711
17	Phillips	Palm 1	50103203610000	4354.50	4354.50	1	410
18	ConocoPhillips	Putu 2A	50103207630100	4291.40	4717.00	119	1531
19	Repsol	Qugruk 8	50103207010000	3834.00	4297.15	103	1091
20	Husky	Seabee 1	50287200070000	270.00	2120.00	7	6564
21	US Navy	Square Lake 1	50119100070000	1646.00	3894.00	54	6004
22	ConocoPhillips	Tinmiaq 2	50103207300000	3311.00	3766.50	45	1650
23	ConocoPhillips	Tinmiaq 6	50103207310000	2450.00	3824.00	56	1418
24	US Navy	Topagoruk 1	50279100330000	302.00	2097.00	10	2748
25	BP	Trailblazer A1	50103203640000	2972.00	3454.00	4	1402
26	BP	Trailblazer H1	50103203690000	2760.00	3090.00	3	1525
27	Texaco	Tulugak 1	50057200010000	1460.00	2540.00	4	8030
28	Husky	Tunalik 1	50301200010000	3288.00	5560.60	3	3036
29	Union	Tungak Creek 1	50207200020000	3067.00	4661.00	10	4979
30	Linc	Umiat 18	50287200280000	714.40	1011.90	72	6485
31	US Navy	Umiat Test 1	50287100010000	1335.00	2996.00	6	6614
32	US Navy	Umiat Test 2	50287100020000	413.00	969.00	4	6469
33	US Navy	Umiat Test 7	50287100070000	834.00	1370.00	5	6543
34	US Navy	Umiat Test 8	50287100080000	507.00	711.00	2	6374
35	US Navy	Umiat Test 11	50287100110000	2078.00	3004.00	37	6301
36	US DOI	Wainwright 1	50301200030000	181.15	1501.45	51	2762
37	US Navy	Wolf Creek 2	50119100090000	2511.00	3520.00	20	7071
38	US Navy	Wolf Creek 3	50119100100000	1533.00	3520.00	78	7191

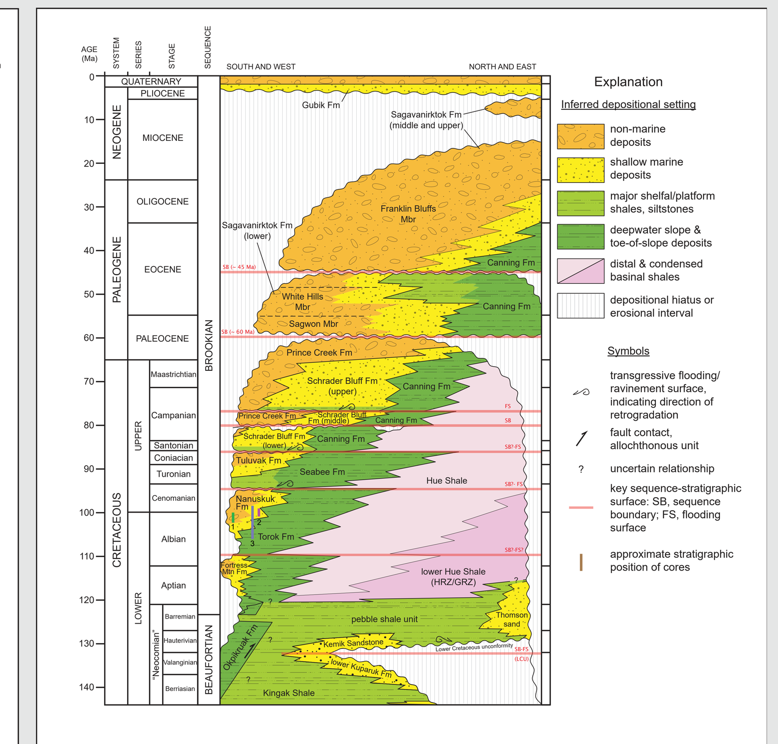

Figure 2. Generalized stratigraphy of the Brookian sequence, central North Slope, Alaska illustrating the stratigraphic position of the Nanushuk Formation. The Kingak Shale, Kemik sandstone, and pebble shale unit comprise the Beaufortian sequence. The approximate stratigraphic positions of cores addressed in this study are shown by vertical lines: green line (1)—Wainwright 1, magenta line (2)—Umiat 18, purple line (3)—Grandstand 1. Modified from Mull and others (2003), Garrity and others (2005), Decker (2010), and Gillis and others (2014). Abbreviations as follows: Fm = Formation, Mbr = Member, Mtn = Mountain, HRZ = Highly radioactive zone, GRZ = Gamma-ray zone.

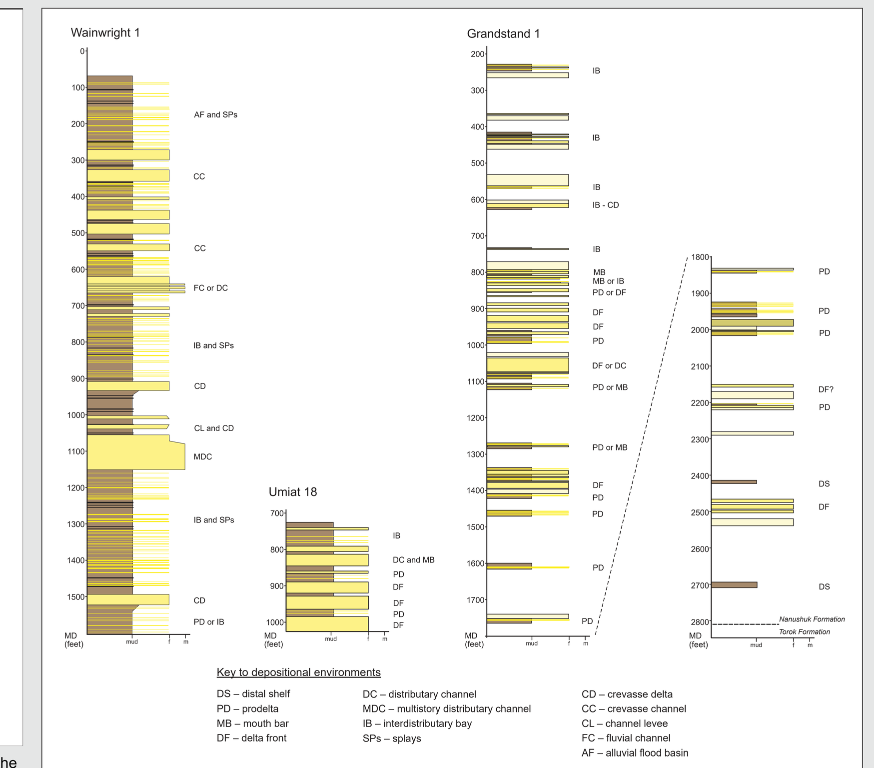

Figure 3. Simplified core descriptions for Wainwright 1, Umiat 18, and Grandstand 1. Measured depth is shown in feet below Kelly bushing; Wainwright 1 and Grandstand 1 are vertical, Umiat 18 is slightly deviated. Yellow is sandstone; pale yellow shows sandstone inferred from cuttings in uncored intervals; brown is siltstone, mudstone, and shale; black is coal; blank areas correspond to uncored intervals in Grandstand 1. Detailed core description of Wainwright 1 is in LePain and Decker (2016); detailed core descriptions of Umiat 18 and Grandstand 1 are in LePain and Helmold (2021). Abbreviation: MD = measured depth.

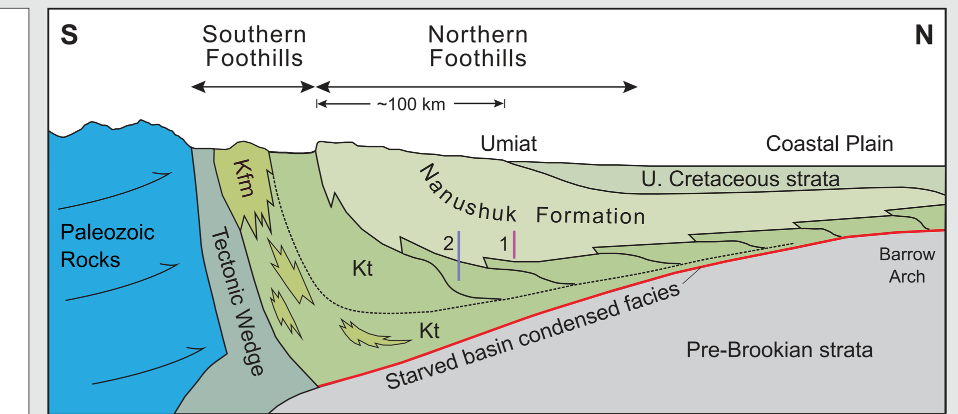

Figure 4. Generalized north–south cross-section through the Colville basin at the approximate longitude of Umiat (line AA' in fig. 1) showing the gross stratal geometries of Lower Cretaceous Brookian formations. The approximate stratigraphic positions of the Umiat 18 and Grandstand 1 cores are shown by vertical lines: magenta line (1)—Umiat 18, purple line (2)—Grandstand 1. Wainwright 1 is not shown due to its location 200 miles northwest of line AA' in fig. 1. Abbreviations as follows: Kfm = Fortress Mountain Formation, Kt = Torok Formation. Modified from Mull (1985) and Houseknecht and Schenk (2001).

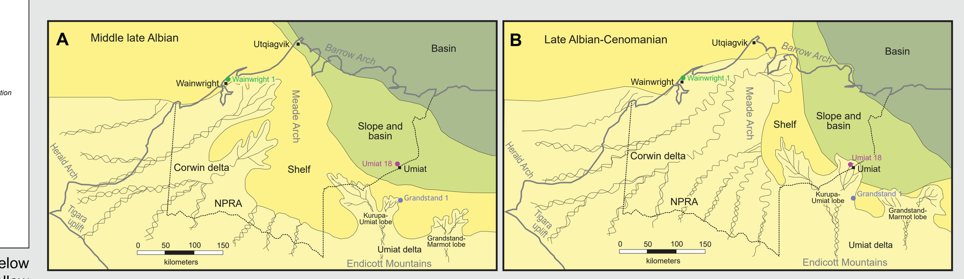

Figure 5. Paleogeographic reconstruction of the central and western Colville basin during (A) middle to late Albian time and (B) late Albian to Cenomanian time. Diagrams show schematic representation of the Corwin delta west of the Meade arch and the Umiat delta, including the Kurupa–Umiat and Grandstand–Marmot lobes, east of the arch. Modified from LePain and others (2009) and Huffman and others (1985).

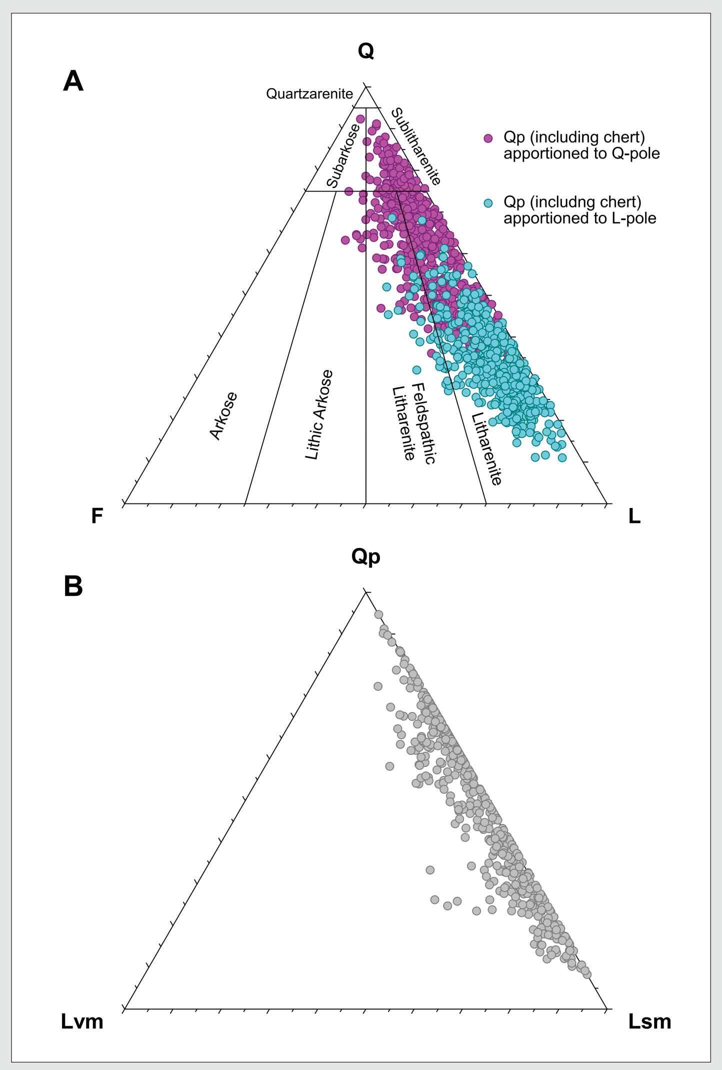

Figure 6. Ternary diagrams displaying detrital composition of Nanushuk sandstone and siltstone. The data were obtained via the traditional point-counting method in which phaneritic rock fragments are classified by their lithology (for example, granite, diorite, gabbro, gneiss). (A) QFL diagram (combination of QtFL and QmFLt diagrams) shows composition of the major detrital grains. When Qp (including chert) is apportioned to the Q-pole, the diagram is a QtFL plot emphasizing grain stability (Dickinson and Suczek, 1979; Dickinson, 1985). When apportioned to the L-pole, the diagram is a QmFLt plot emphasizing provenance. In either case, Nanushuk sandstone is primarily a litharenite. Sandstone classification scheme of Folk, 1974. (B) QpLvmLsm diagram details composition of the lithic grains which consist largely of polycrystalline quartz (predominantly chert) and argillaceous sedimentary and metasedimentary rock fragments. The ductility of argillaceous rock fragments plays a crucial role in diagenesis due to their deformation with burial resulting in loss of reservoir quality.

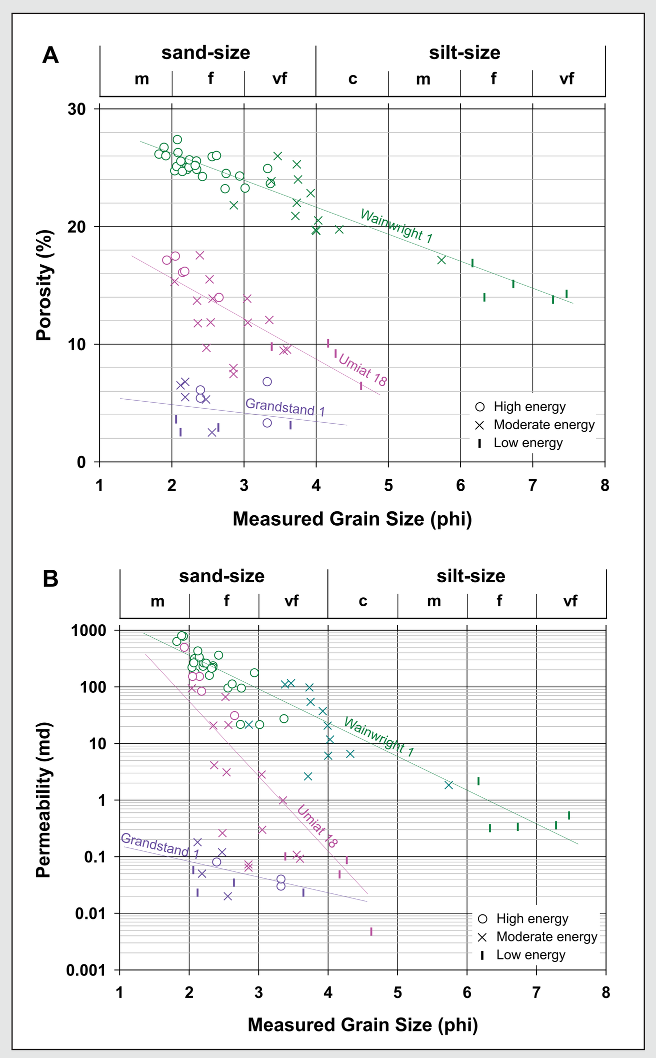

Figure 7. Cross-plots of porosity and permeability versus grain size for Wainwright 1 (low Dmax), Umiat 18 (moderate Dmax), and Grandstand 1 (high Dmax) wells in which data are coded by strength of depositional energy. The energy of depositional environments is classified as: high-energy = distributary channel and distributary mouth bar; moderate-energy = delta front, crevasse channel, shoreface, and abandoned distributary channel; low-energy = bayfill, prodelta, interdistributary bay, channel levee, and crevasse delta. There is overlap between some environments classified as moderate energy (shoreface) and high energy (distributary channel and channel mouth bar); some Nanushuk shoreface deposits were shaped by high-energy storm waves. This elucidates the nexus between environments of deposition, depositional energy, and grain size, and is important in establishing depositional texture as the primary, local control on reservoir quality. Deposits of high-energy currents are predominantly fine-grained sandstone, deposits of moderate-energy currents are chiefly very fine- and fine-grained sandstone, and deposits of low-energy currents are typically siltstone. The ranges of porosity and permeability values for Grandstand 1 are constricted due to the greater degree of compaction. (A) Plot of porosity (%) versus grain size (phi). (B) Plot of permeability (md) versus grain size (phi).

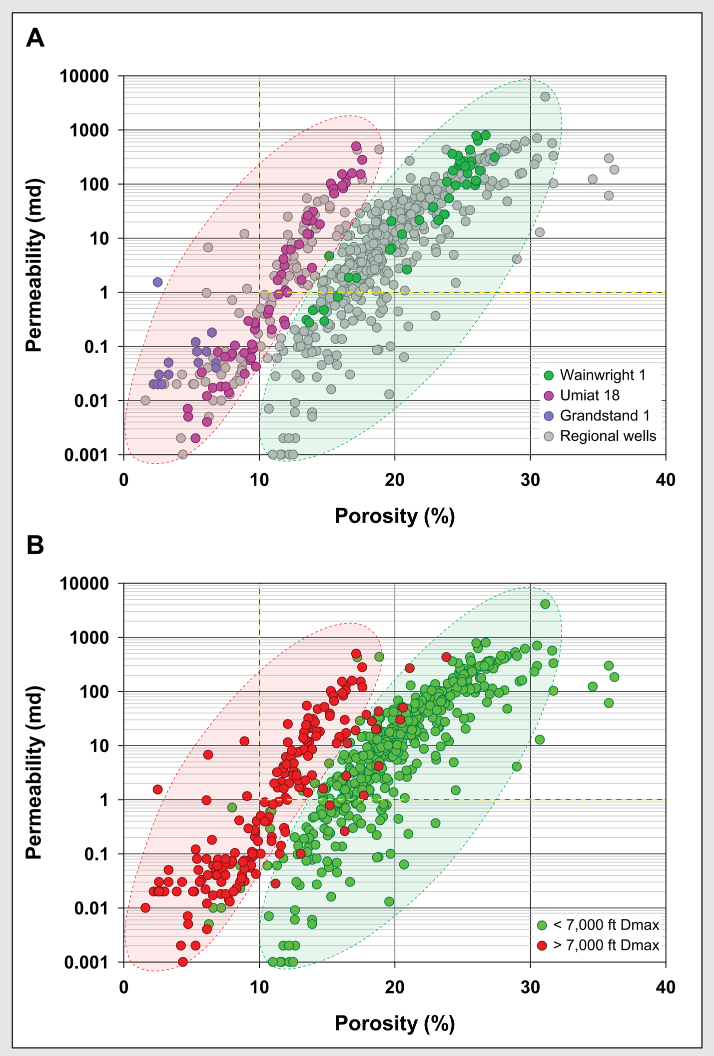

Figure 8. Porosity–permeability cross-plots displaying two groups with parallel trends in reservoir quality. A low-porosity group has maximum porosity less than 20 percent (red dashed oval); a high-porosity group has higher porosity values for a given permeability, with maximum porosity exceeding 30 percent (green dashed oval). Yellow dashed lines mark the informal limits for producible Brookian reservoirs: 10 percent porosity and 1 md permeability. (A) Samples are coded by well. Wainwright 1 is characteristic of the better reservoir-quality rock subjected to shallow burial, while Umiat 18 and Grandstand 1 are characteristic of the poorer reservoir-quality rock subjected to moderate to deep burial, respectively. (B) Same plot as A with samples coded by Dmax. Most samples in the low-porosity group (red oval) have a Dmax greater than 7,000 ft, while most within the high-porosity group (green oval) have a Dmax less than 7,000 ft. This supports the interpretation that the two groups result from differences in burial.

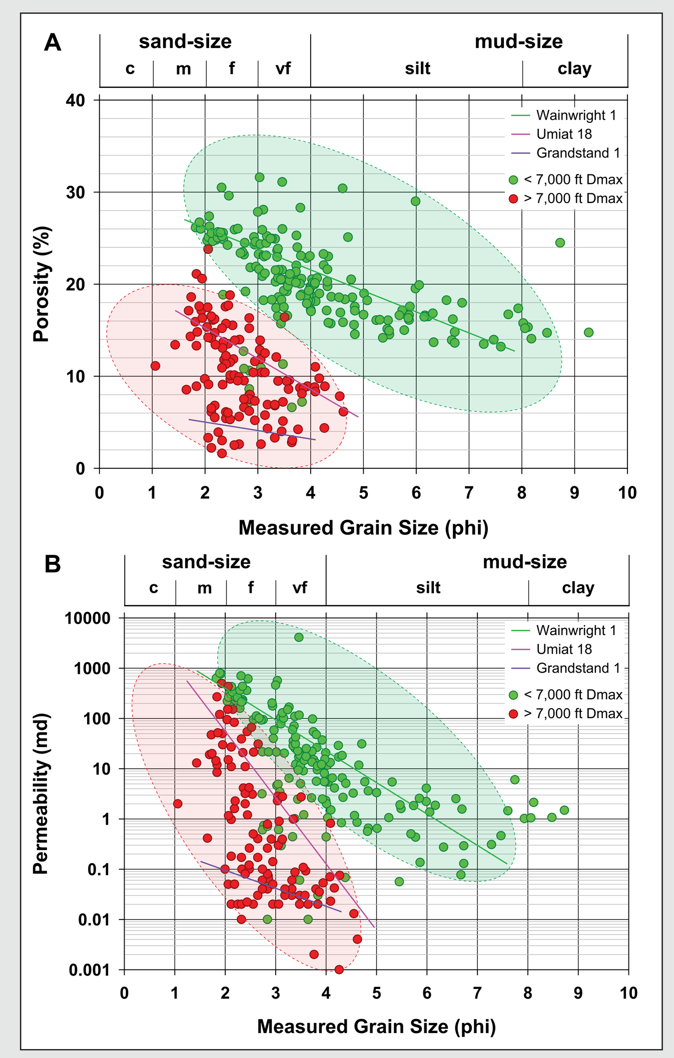

Figure 9. Cross-plots of porosity and permeability versus grain size. (A) Porosity–grain size plot showing two groups with parallel trends. One group includes rocks with Dmax less than 7,000 ft (green dashed oval), the other contains rocks with Dmax greater than 7,000 ft (red dashed oval). Wainwright 1 (green regression line) is representative of shallow burial, Umiat 18 (magenta regression line) and Grandstand 1 (purple regression line) are of characteristic of moderate to deep burial, respectively. The two groups mimic those characteristic of the porosity–permeability relation (fig. 8). (B) Permeability–grain size plot with groups comparable to those displayed in porosity–grain size plot (A).

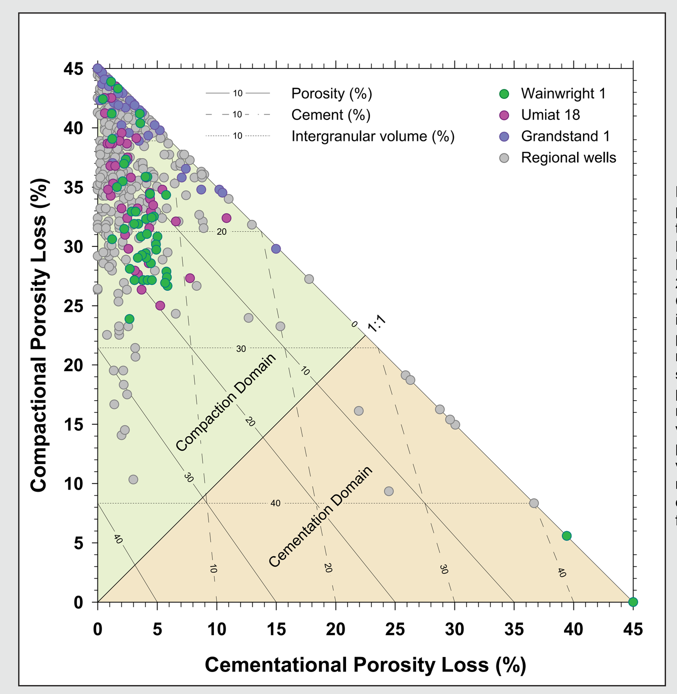

Figure 10. Cross-plot of compactional porosity loss (COPL) versus cementational porosity loss (CEPL) for Nanushuk sandstone and siltstone. Most samples have COPL values of 25–45 percent with corresponding CEPL values less than 10 percent indicating mechanical compaction plays a much larger role in porosity reduction than cementation. Sandstones with CEPL greater than 45 percent are set to the assumed maximum depositional intergranular volume of 45 percent. Lines of equal porosity, cement, and intergranular volume are shown; diagonal line (1:1) represents equal porosity loss by compaction and cementation. Modified from Lundegard (1992).

Table 2. Linear regression models to predict porosity and permeability of Nanushuk sandstone and siltstone from maximum burial depth (Dmax). The analyses use all available porosity, permeability, and Dmax data (full-dataset model); samples with greater than 10 percent carbonate cement are excluded (fig. 12). When applied to pre-drill predictions, an estimate of the maximum burial depth of the prospective reservoir yields predictions for the mean values of core porosity and permeability. The ranges of porosity and permeability values expected in cores are estimated by the means ± 1 σ. Coefficient of porosity intercept = 35.8166, coefficient of porosity slope = -0.00301648, coefficient of log(permeability) intercept = 2.57678, coefficient of log(permeability) slope = -0.000315919, porosity 1 σ = 7.3088, log(permeability) 1 σ = 1.32159.

Full-Dataset Model						
	Porosity Regression			Permeability Regression		
Dmax	Porosity	Porosity - 1 σ	Porosity + 1 σ	Permeability	Permeability - 1 σ	Permeability + 1 σ
1,000	32.8	25.5	40.1	182.331	8.695	3823.411
2,000	29.8	22.5	37.1	88.093	4.201	1847.277
3,000	26.8	19.5	34.1	42.562	2.030	892.510
4,000	23.8	16.4	31.1	20.564	0.981	431.215
5,000	20.7	13.4	28.0	9.935	0.474	208.341
6,000	17.7	10.4	25.0	4.800	0.229	100.660
7,000	14.7	7.4	22.0	2.319	0.111	48.634
8,000	11.7	4.4	19.0	1.121	0.053	23.497
9,000	8.7	1.4	16.0	0.541	0.026	11.353
10,000	5.7	0.0	13.0	0.262	0.012	5.485
11,000	2.6	0.0	9.9	0.126	0.006	2.650
12,000	0.0	0.0	7.3	0.061	0.003	1.280
13,000	0.0	0.0	7.3	0.030	0.001	0.619
14,000	0.0	0.0	7.3	0.014	0.001	0.299

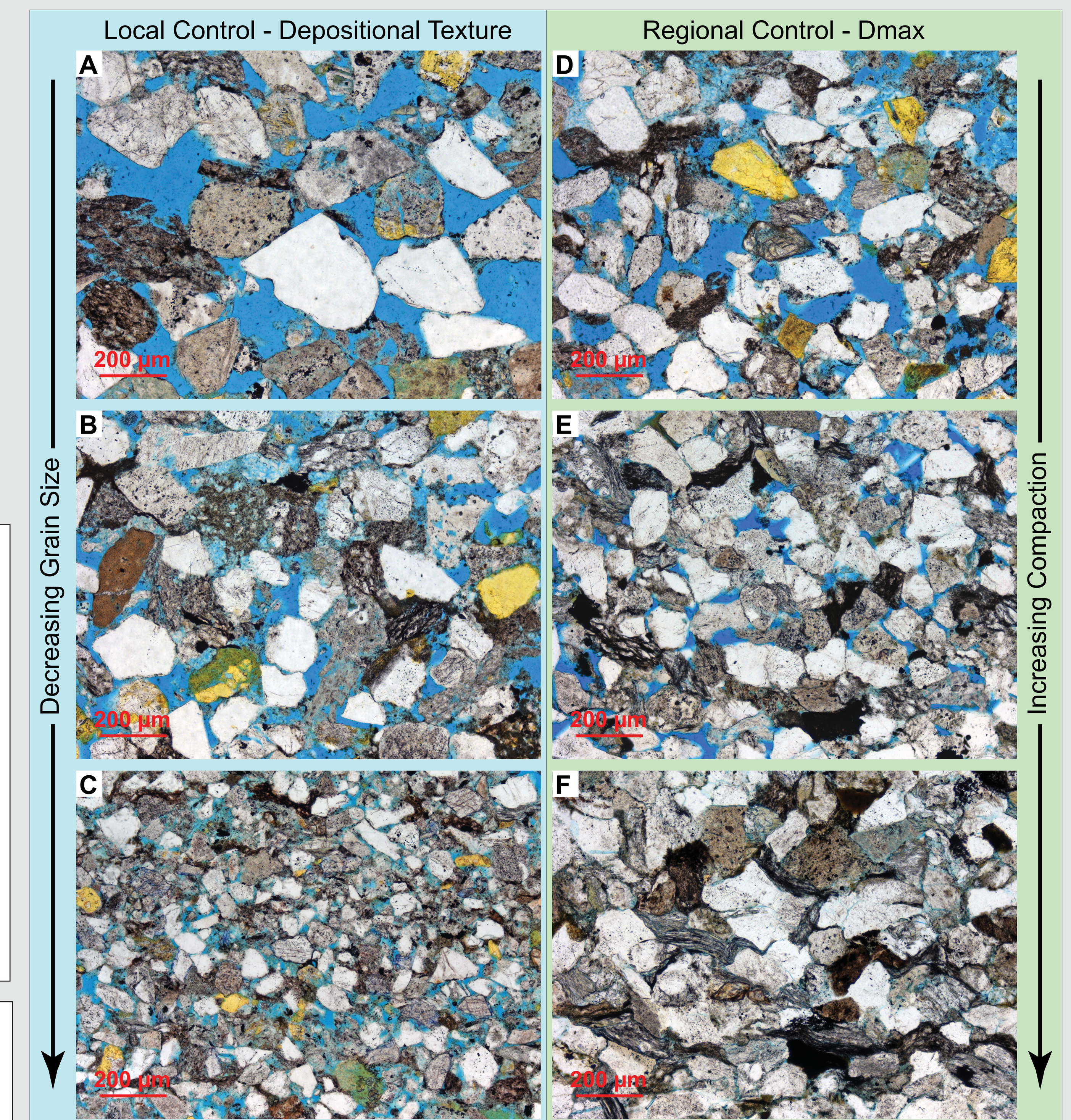

Figure 11. Photomicrographs contrasting petrographic characteristics of Nanushuk sandstone in which reservoir quality is controlled by depositional texture (A–C) to those in which maximum burial depth is the dominant control (D–F). All images were acquired at the same magnification to directly compare grain size. Sandstones in A–C have similar values of Dmax (mean 3,715 ft) but differ in grain size, varying from medium- (A) to very fine-grained sand (C). The decrease in grain-size positively correlates with reservoir quality, best illustrated by permeability, which decreases from 796.2 md in the medium-grained sandstone (A) to 20.7 md in the very fine-grained rock (C). Grain size is a proxy for depositional texture which exerts a primary, local control on reservoir quality. Sandstones in D–F have similar grain size (mean 2.53 phi, fine-grain sand), but widely different values of Dmax, varying from 3,424 ft (D) to 8,884 ft (F). The increase in Dmax negatively correlates with reservoir quality, with permeabilities decreasing from 112.0 md in the more shallowly buried sandstone (D) to 0.08 md in the more deeply buried rock (F). This illustrates the secondary, regional control that maximum burial depth has on reservoir quality. (A) Medium-grained sandstone with 26.7% porosity, 796.2 md permeability, and 3890.1 ft Dmax; Wainwright 1, 1128.1 ft MD; plane-polarized light. (B) Fine-grained sandstone with 25.9% porosity, 95.0 md permeability, and 3420.15 ft Dmax; Wainwright 1, 658.15 ft MD; plane-polarized light. (C) Very fine-grained sandstone with 19.7% porosity, 20.7 md permeability, and 3834.1 ft Dmax; Wainwright 1, 1072.1 ft MD; plane-polarized light. (D) Fine-grained sandstone with 26.0% porosity, 112.0 md permeability, and 3424.15 ft Dmax; Wainwright 1, 662.15 ft MD; plane-polarized light. (E) Fine-grained sandstone with 13.9% porosity, 21.3 md permeability, and 7364.5 ft Dmax; Umiat 18, 879.5 ft MD; plane-polarized light. (F) Fine-grained sandstone with 5.4% porosity, 0.08 md permeability, and 8883.5 ft Dmax; Grandstand 1, 799.5 ft MD; plane-polarized light. Abbreviation: MD = measured depth.

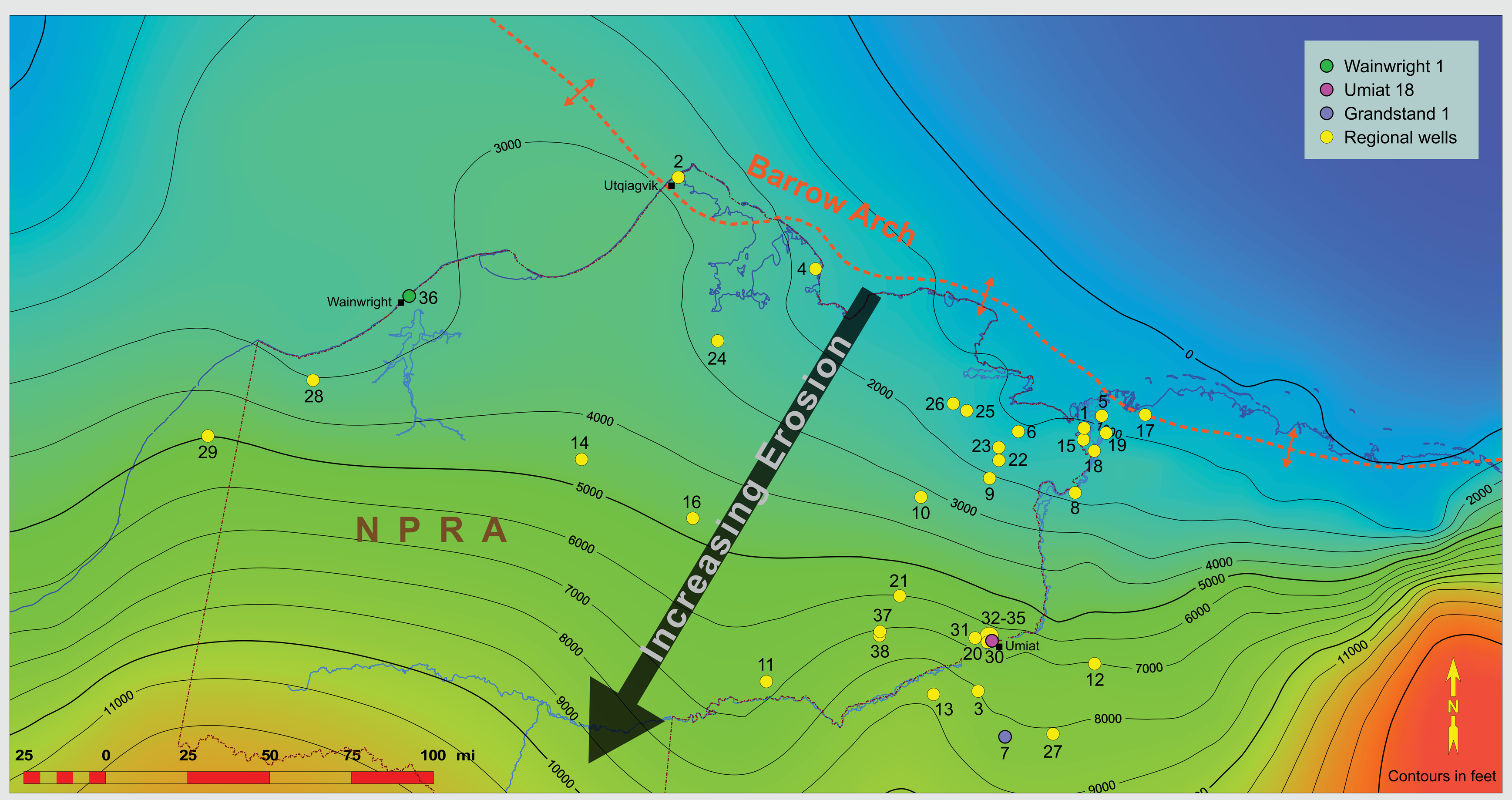

Figure 12. Map of the central North Slope with contours (in ft) of estimated thickness of exhumed Brookian strata. Numbered yellow dots correspond to 38 wells listed in table 1; three key wells (36–Wainwright 1, 30–Umiat 18, and 7–Grandstand 1) are highlighted. The large arrow shows the regional trend of increasing amount of erosion to the south. Contours were generated from exhumation estimates at 145 wellsites (Burns and others, 2007) using GeoAtlas, the mapping module of GeoGraphix.

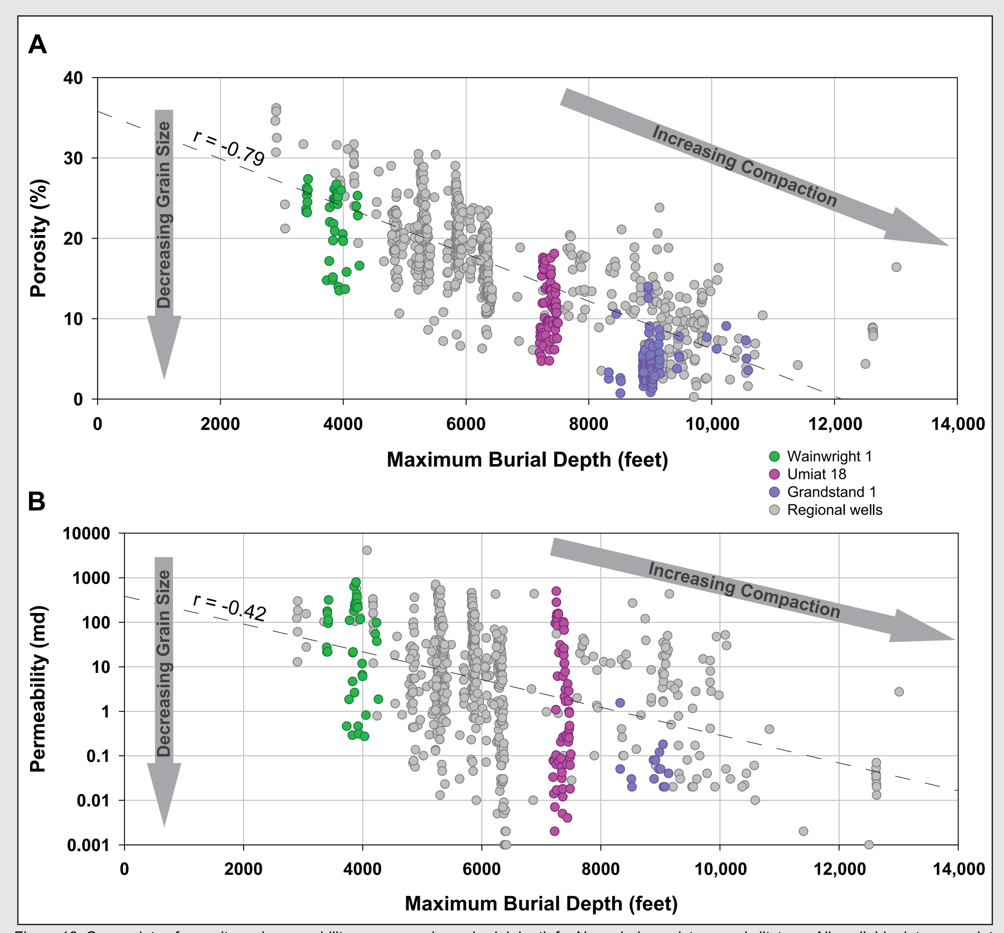

Figure 13. Cross-plots of porosity and permeability versus maximum burial depth for Nanushuk sandstone and siltstone. All available data were plotted (compare with fig. 14) except for samples with greater than 10 percent carbonate cement. The arrows depict the two major controls on reservoir quality: depositional texture (grain size as proxy) and compaction. For any given value of Dmax, intra-well variability in porosity and permeability is largely controlled by depositional texture as signaled by grain size. At the regional scale, values of porosity and permeability, and their intra-well variation, are reduced with increasing Dmax due to greater compaction of the sandstone. (A) Porosity versus Dmax plot. Wainwright 1 (~4,000 ft Dmax) is indicative of shallow burial while Umiat 18 (~7,000 ft Dmax) and Grandstand 1 (~9,000 ft Dmax) are representative of moderately to deeply buried rocks, respectively. (B) Permeability versus Dmax plot. Permeability has a larger standard deviation than porosity.

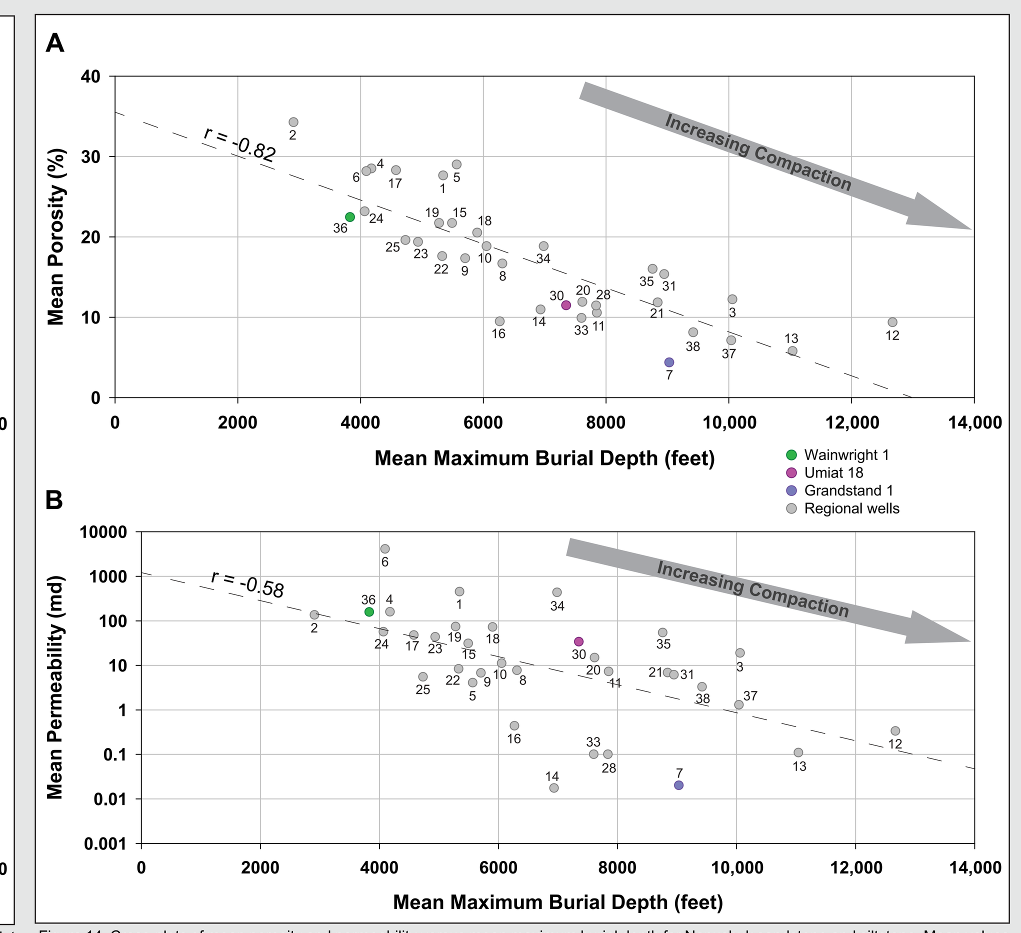

Figure 14. Cross-plots of mean porosity and permeability versus mean maximum burial depth for Nanushuk sandstone and siltstone. Mean values are plotted by well (compare with fig. 13); samples with greater than 10 percent carbonate cement were excluded from the means. The arrow depicts the secondary, regional compaction control has on reservoir quality; the role of depositional texture, as indicated by grain size, is not evident from plots of mean values. Correlation coefficients are greater than for plots incorporating all the data (fig. 13), but complexity of the data is hidden. Numbered gray dots correspond to 38 wells listed in table 1; three key wells (36–Wainwright 1, 30–Umiat 18, and 7–Grandstand 1) are highlighted. (A) Mean porosity versus mean Dmax plot. (B) Mean permeability versus mean Dmax plot.

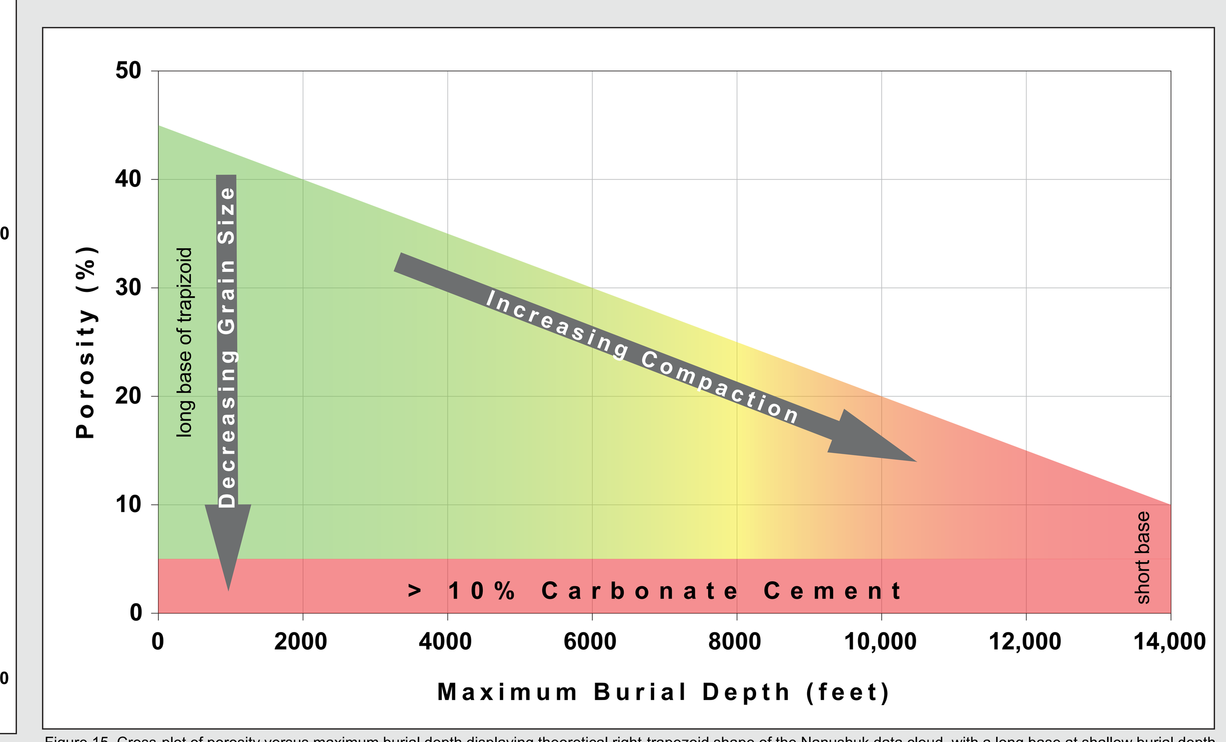

Figure 15. Cross-plot of porosity versus maximum burial depth displaying theoretical right-trapezoid shape of the Nanushuk data cloud, with a long base at shallow burial depth and a short base at deep burial depth. [Note on terminology: a right trapezoid is a convex quadrilateral with one pair of parallel sides and two adjacent right angles. The parallel sides are the bases of the trapezoid, while the non-parallel sides are the legs.] Highly cemented sandstone with greater than 10 percent carbonate cement occurs as a narrow band with low porosity along the right-angle leg of the trapezoid. The green–yellow–red shading represents the relative extent of reservoir quality; a value of ~8,000 ft Dmax marks the approximate boundary between productive and non-productive Nanushuk reservoirs. The arrows signify the primary, local (depositional texture) and secondary, regional (compaction) controls on reservoir quality. A cross-plot of permeability versus Dmax should have a similar theoretical distribution of data.

ACKNOWLEDGMENTS

The Alaska Geologic Materials Center provided thin sections from the Fish Creek 1, Square Lake 1, Grandstand 1, and Wolf Creek 3 wells; the assistance of Kurt Johnson and Jean Riordan is greatly appreciated. David Houseknecht and Kenneth Bird provided the routine core analyses and core plug trim-ends from the Wainwright 1 well. Corri Feige was instrumental in gaining access to material and data from the Umiat 18 core. Linc Energy granted access to thin sections and routine core analyses from the core and Leonard Sojka facilitated the loan of this material to DGGS/DOG. Discussions with Stephen Franks, Richard Garrard, Gregory Wilson, Paul Decker, and John Decker helped develop the concepts documented in this poster. The senior author gained valuable experience forecasting reservoir quality of Brookian sandstone while employed by ARCO Oil & Gas Company and ARCO Alaska, Inc. that proved indispensable in this study.

Alaska Department of Natural Resources

Alaska Division of Geological & Geophysical Surveys
Alaska Division of Oil & Gas